Angewandte International Edition Chemie

Editorial

C. L. Raston* ——— 10676 – 10677

Australian Chemistry under the Spotlight

"... The big challenge is to ensure that the country invests in science and technology for the future, to eventually deal with the challenges once the mining boom is over ..." Read more in the Editorial by Colin L. Raston.

Service

Spotlight on Angewandte's Sister Journals ***10694 – 10696***

Author Profile

Julius Rebek, Jr. ——— 10698 – 10699

"If I won the lottery, I would keep doing chemistry. My favorite place on earth is the VIth district of Paris ..." This and more about Julius Rebek, Jr. can be found on page 10698.

News

International Biannual Belgian Polymer Group Award: C. Barner-Kowollik **10700**

Election to the Bavarian Academy of Science and Humanities: H.-U. Reissig ——— **10700**

Civic Medal First Class and Honorary Doctorate: G. Bringmann ——— **10700**

C. Barner-Kowollik

H.-U. Reissig

G. Bringmann

Books

Organic Chemistry David R. Klein *reviewed by A. K. Franz* ——— **10701**

Highlights

5-Hydroxymethylcytosine

P. Schüler, A. K. Miller* — 10704 – 10707

Sequencing the Sixth Base (5-Hydroxymethylcytosine): Selective DNA Oxidation Enables Base-Pair Resolution

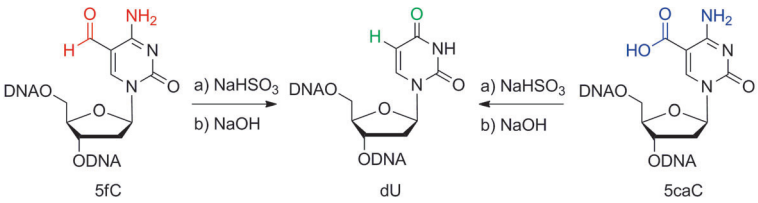

Sodium bisulfite promotes both the deformylative deamination of 5-formylcytosine (5fC) and the decarboxylative deamination of 5-carboxylcytosine (5caC; see picture). By coupling this bisulfite chemistry with selective oxidations of individual DNA bases, new methods allow, for the first time, the sequencing of 5-hydroxymethylcytosine (5hmC) with single-base-pair resolution.

Materials Science

S. K. Prasad* — 10708 – 10710

Photostimulated and Photosuppressed Phase Transitions in Liquid Crystals

Shape matters: Changes, which are brought about by irradiation, to the properties of a medium have been of immense interest not only in terms of basic science, but also for applications such as data storage media and molecular devices. In the light of a recent publication reporting a photodriven liquid to liquid crystalline transformation (see figure), an overview of similar transitions is presented.

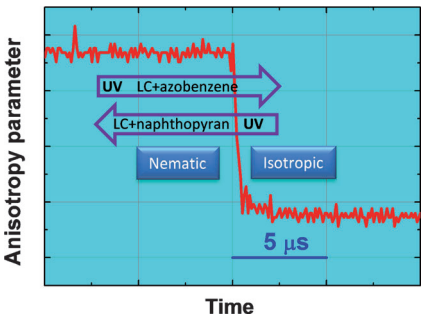

Minireviews

C–H Bond Activation

M. Bordeaux, A. Galarneau, J. Drone* — 10712 – 10723

Catalytic, Mild, and Selective Oxyfunctionalization of Linear Alkanes: Current Challenges

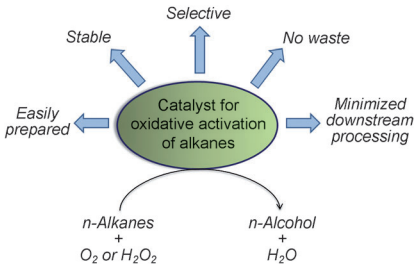

Seeking ideality: Intensive efforts have been invested into the discovery and/or engineering of a range of catalysts, ideally meeting the criteria shown in the picture, for the oxidative C–H bond activation of linear alkanes. The comparison between chemical and enzymatic catalysts for alkane oxyfunctionalization is an extremely useful strategy to gain insights into the fundamental mechanisms of this chemistry.

For the USA and Canada:
ANGEWANDTE CHEMIE International Edition (ISSN 1433-7851) is published weekly by Wiley-VCH, PO Box 191161, 69451 Weinheim, Germany. Air freight and mailing in the USA by Publications Expediting Inc., 200 Meacham Ave., Elmont, NY 11003. Periodicals postage paid at Jamaica, NY 11431. US POSTMASTER: send address changes to *Angewandte Chemie*, Journal Customer Services, John Wiley & Sons Inc., 350 Main St., Malden, MA 02148-5020. Annual subscription price for institutions: US$ 11.738/10.206 (valid for print and electronic / print or electronic delivery); for individuals who are personal members of a national chemical society prices are available on request. Postage and handling charges included. All prices are subject to local VAT/sales tax.

Reviews

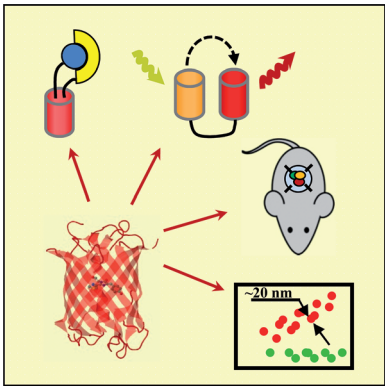

Well red: Modern red fluorescent proteins (RFPs) provide new possibilities to study biological processes at the levels from single molecules to whole organisms (see scheme). Conventional and far-red RFPs, RFPs with a large Stokes shift, fluorescent timers, irreversibly photoactivatable, and reversibly photoswitchable RFPs are discussed in relationship to advanced imaging approaches.

Imaging Agents

D. M. Shcherbakova, O. M. Subach, V. V. Verkhusha* ——— **10724 – 10738**

Red Fluorescent Proteins: Advanced Imaging Applications and Future Design

Communications

Pencil it in: Mechanical abrasion of compressed single-walled carbon nanotubes (SWCNTs) on the surface of paper produces sensors capable of detecting NH_3 gas at sub-ppm concentrations. This method of fabrication is simple, inexpensive, and entirely solvent-free, and avoids difficulties arising from the inherent instability of many SWCNT dispersions.

Gas Sensors

K. A. Mirica, J. G. Weis, J. M. Schnorr, B. Esser, T. M. Swager* ——— **10740 – 10745**

Mechanical Drawing of Gas Sensors on Paper

Frontispiece

A polymersome-stabilized Pickering emulsion was prepared and applied in a biphasic enzymatic reaction. This type of Pickering emulsion was stabilized by fully packed crosslinked polymersomes at the water/oil interface. CalB, as a model enzyme (red ribbon structure), was loaded either in the water phase or in the lumen of the polymersomes of the Pickering emulsion (see picture), which highly enhanced its catalytic performance and recyclability.

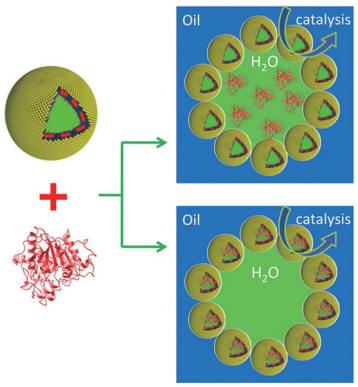

Biocatalytic Nanoreactors

Z. Wang, M. C. M. van Oers, F. P. J. T. Rutjes, J. C. M. van Hest* ——— **10746 – 10750**

Polymersome Colloidosomes for Enzyme Catalysis in a Biphasic System

Inside Back Cover

The German Chemical Society (GDCh) invites you to:

Angewandte Anniversary Symposium

125 JAHRE Eine Zeitschrift der Gesellschaft Deutscher Chemiker

GDCh

Tuesday, March 12, 2013

Henry Ford Building / FU Berlin

Speakers

Carolyn R. Bertozzi

François Diederich

Alois Fürstner

Roald Hoffmann (Nobel Prize 1981)

Susumu Kitagawa

Jean-Marie Lehn (Nobel Prize 1987)

E.W. "Bert" Meijer

Frank Schirrmacher (Publisher, *FAZ*)

Robert Schlögl

George M. Whitesides

Ahmed Zewail (Nobel Prize 1999)

More information:

Freie Universität Berlin

angewandte.org/symposium

WILEY-VCH

GDCh Gesellschaft Deutscher Chemiker

PSJ_12_42497_5_gu

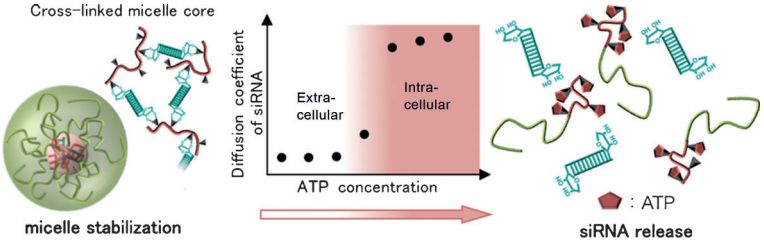

PIC-ing a winner: siRNA encapsulated by a phenylboronate-functionalized polyion complex (PIC) micelle shows binding between the phenylboronate and the 3′ ribose of the siRNA (see scheme), stabilizing the complex under conditions equivalent to the extracellular environment. This complex is disrupted in response to addition of ATP, at a concentration comparable to that inside cells.

siRNA Delivery

M. Naito, T. Ishii, A. Matsumoto, K. Miyata, Y. Miyahara, K. Kataoka* _____ **10751 – 10755**

A Phenylboronate-Functionalized Polyion Complex Micelle for ATP-Triggered Release of siRNA

Back Cover

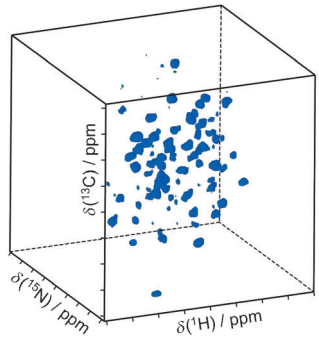

Narrow ^{1}H NMR linewidths can be obtained for fully protonated protein samples in the solid state by using ultrafast magic-angle spinning (60 kHz). Medium-size microcrystalline and non-crystalline proteins can be analyzed without any need for deuteration of the protein sample. This approach provides assignments of the backbone ^{1}H, ^{15}N, ^{13}C$^\alpha$, and ^{13}CO resonances and yields information about ^{1}H–^{1}H proximities.

Solid-State Protein NMR Spectroscopy

A. Marchetti, S. Jehle, M. Felletti, M. J. Knight, Y. Wang, Z.-Q. Xu, A. Y. Park, G. Otting, A. Lesage, L. Emsley, N. E. Dixon, G. Pintacuda* _____ **10756 – 10759**

Backbone Assignment of Fully Protonated Solid Proteins by ^{1}H Detection and Ultrafast Magic-Angle-Spinning NMR Spectroscopy

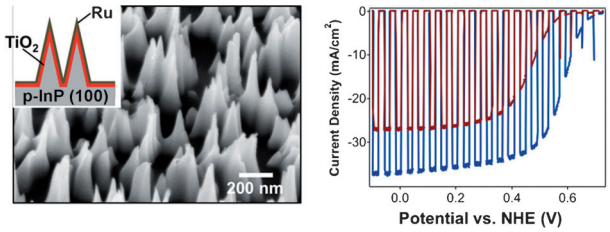

Perfect texture: The roles of surface nanotexturing, TiO_2 passivation, and a ruthenium cocatalyst on the photoelectrochemical evolution of hydrogen by using p-InP photocathodes are investigated. Higher current densities and more favorable onset potentials are observed after surface nanotexturing. NHE = normal hydrogen electrode.

Water Splitting

M. H. Lee, K. Takei, J. Zhang, R. Kapadia, M. Zheng, Y.-Z. Chen, J. Nah, T. S. Matthews, Y.-L. Chueh, J. W. Ager,* A. Javey* _____ **10760 – 10764**

p-Type InP Nanopillar Photocathodes for Efficient Solar-Driven Hydrogen Production

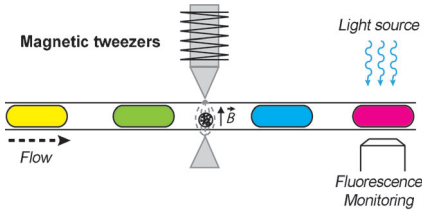

Tweezing out the answer: A microfluidic device combining droplets (less than 100 nL) and magnetic particles (see scheme) was implemented for fast heterogeneous multiplexed assays. Magnetic tweezers can perform the manipulations required in an immunoassay (capture, extraction, mixing, and rinsing). This method was applied to the diagnosis of congenital hypothyroidism with 14 pM sensitivity.

Microfluidic Bioassay

A. Ali-Cherif, S. Begolo, S. Descroix, J.-L. Viovy, L. Malaquin* _ **10765 – 10769**

Programmable Magnetic Tweezers and Droplet Microfluidic Device for High-Throughput Nanoliter Multi-Step Assays

Functional Materials

M. R. Dolgos, U. Adem, A. Manjon-Sanz, X. Wan, T. P. Comyn, T. Stevenson, J. Bennett, A. J. Bell, T. T. Tran, P. S. Halasyamani, J. B. Claridge,* M. J. Rosseinsky* _____ **10770 – 10775**

Perovskite B-Site Compositional Control of $[110]_p$ Polar Displacement Coupling in an Ambient-Pressure-Stable Bismuth-based Ferroelectric

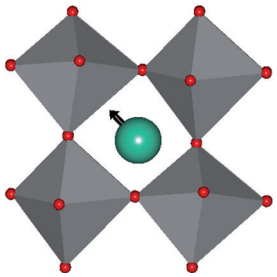

Off the axis: A new lead-free bismuth based perovskite has been formed at ambient pressure in the polar $Pmc2_1$ structure. Measurements give evidence for ferroelectricity and piezoelectricity. The material is significant due to a rotation of the polarization direction off the $[111]_p$ axis, making it important to the design of materials with a morphotropic phase boundary.

Nanoparticles Self-Assembly

P. Simon,* E. Rosseeva, I. A. Baburin, L. Liebscher, S. G. Hickey, R. Cardoso-Gil, A. Eychmüller, R. Kniep, W. Carrillo-Cabrera _____ **10776 – 10781**

PbS–Organic Mesocrystals: The Relationship between Nanocrystal Orientation and Superlattice Array

Try to make it ordered! Micrometer-sized PbS–organic mesocrystals show a long-range order of nanoparticles within an *fcc* superlattice combined with preferred orientational ordering of truncated octahedrally shaped PbS cores (see picture). The concept of formation and structuring of mesocrystalline materials is perfectly illustrated this system.

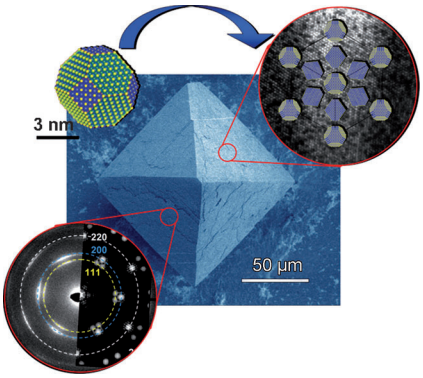

Photoluminescence

Y. J. Dong, B. Xu, J. B. Zhang, X. Tan, L. J. Wang, J. L. Chen, H. G. Lv, S. P. Wen, B. Li, L. Ye, B. Zou,* W. J. Tian* _____ **10782 – 10785**

Piezochromic Luminescence Based on the Molecular Aggregation of 9,10-Bis((*E*)-2-(pyrid-2-yl)vinyl)anthracene

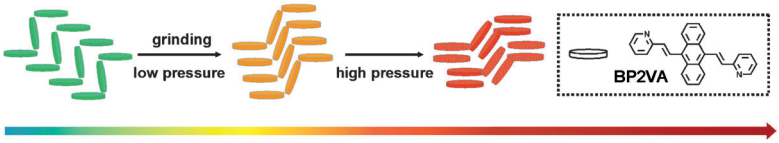

A chameleon under pressure: The observed piezochromic behavior of the title compound (BP2VA) was found to depend on its molecular aggregation state and specifically on the strength of the π–π interaction between the anthracene rings of adjacent molecules. When BP2VA is ground or placed under pressure, its molecular aggregation state changes, and a red shift in the fluorescence emission from green via orange to red occurs (see picture).

Electrocatalysis

T. Hibino,* Y. Shen, M. Nishida, M. Nagao _____ **10786 – 10790**

Hydroxide Ion Conducting Antimony(V)-Doped Tin Pyrophosphate Electrolyte for Intermediate-Temperature Alkaline Fuel Cells

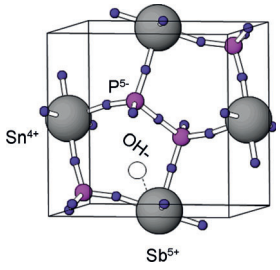

Ion conductor: A series of $Sn_{1-x}A_xP_2O_7$ (A^V = V, Nb, Ta, and Sb) compounds was synthesized, among which $Sn_{0.92}Sb_{0.08}P_2O_7$ (see picture) showed the highest hydroxide ion conductivity in the temperature range of 50–200 °C (0.08 S cm^{-1} at 100 °C and 0.05 S cm^{-1} at 200 °C). This high conductivity was also confirmed under fuel-cell-operating conditions.

Dense metastable phases obtained under "hard" high-pressure conditions may contain instabilities such as unusual oxidation states or coordination environments that may be partially relieved by "soft" low-temperature chemistry. The synthesis of $SrCrO_{2.8}$ (see picture, left) and $SrCrO_{2.75}$ (right) phases from the high-pressure perovskite $SrCrO_3$ leads to a relaxation of the coordination around Cr^{4+} from octahedral to tetrahedral.

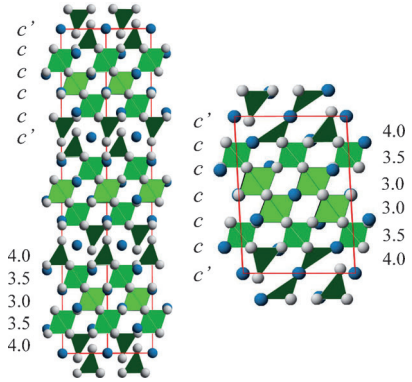

Materials Synthesis

A. M. Arévalo-López, J. A. Rodgers, M. S. Senn, F. Sher, J. Farnham, W. Gibbs, J. P. Attfield* _____ **10791 – 10794**

"Hard–Soft" Synthesis of $SrCrO_{3-\delta}$ Superstructure Phases

Turn it on! β-MAP is a sensitive FRET probe with specificity for monitoring the enzyme β-secretase (BACE), which is associated with Alzheimer's disease. After hydrolysis by the enzyme BACE, the probe fluoresces and thus allows real-time spatial and temporal assessment of enzymatic activity in living cells. β-MAP was used to confirm the cellular efficacy of a reported inhibitor without the need for mutated cell lines or antibodies.

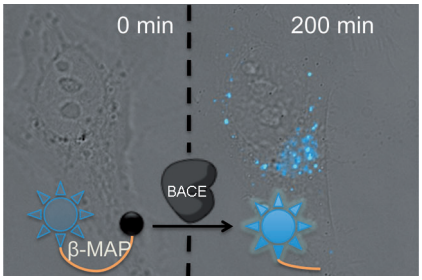

Live-Cell Imaging

D. S. Folk, J. C. Torosian, S. Hwang, D. G. McCafferty, K. J. Franz* _____ **10795 – 10799**

Monitoring β-Secretase Activity in Living Cells with a Membrane-Anchored FRET Probe

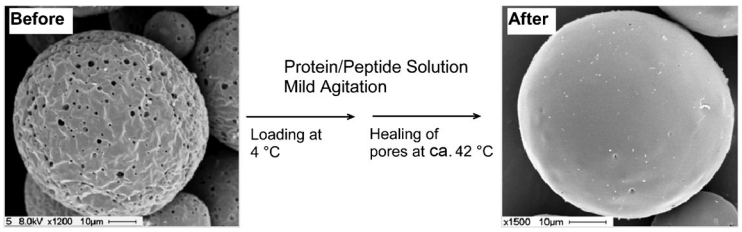

Capture and seal off all exits! Biomacromolecules are routinely microcapsulated in poly(lactic-*co*-glycolic acid) (PLGA) in multiple complex steps that are deleterious to the biomacromolecule. In contrast, PLGA encapsulation based on self-healing (see picture) shows high efficiency without protein damage and enables the stabilization and slow release of proteins.

Protein Stabilization

S. E. Reinhold, K.-G. H. Desai, L. Zhang, K. F. Olsen, S. P. Schwendeman* ____ **10800 – 10803**

Self-Healing Microencapsulation of Biomacromolecules without Organic Solvents

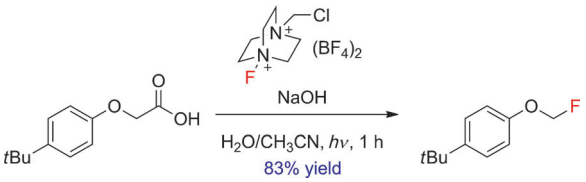

Coming to light: The title reaction simply requires an aqueous alkaline solution of Selectfluor and light. The method is inexpensive and effective for a wide range of neutral and electron-poor 2-aryloxy and 2-aryl acetic acids to provide fluoromethyl ethers (see scheme) and benzyl fluorides, respectively. The mechanism most likely proceeds through an initial aryl excitation with a subsequent single-electron transfer.

Synthetic Methods

J. C. T. Leung, C. Chatalova-Sazepin, J. G. West, M. Rueda-Becerril, J.-F. Paquin, G. M. Sammis* _____ **10804 – 10807**

Photo-fluorodecarboxylation of 2-Aryloxy and 2-Aryl Carboxylic Acids

C–C Coupling

S. Aspin, A.-S. Goutierre, P. Larini, R. Jazzar, O. Baudoin* — 10808 – 10811

Synthesis of Aromatic α-Aminoesters: Palladium-Catalyzed Long-Range Arylation of Primary C_{sp^3}–H Bonds

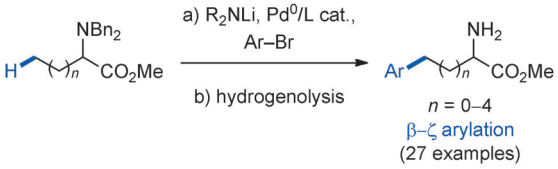

Remote control: The title reaction for β–ζ arylation of α-amino esters with aryl bromides is described. This reaction, which occurs selectively at the terminal position of linear alkyl chains, gives rise to synthetically useful (hetero)arylalanines and homologues after debenzylation (see scheme).

Organometallic Catalysis

Y. Hoshimoto, Y. Hayashi, H. Suzuki, M. Ohashi, S. Ogoshi* — 10812 – 10815

Synthesis of Five- and Six-Membered Benzocyclic Ketones through Intramolecular Alkene Hydroacylation Catalyzed by Nickel(0)/N-Heterocyclic Carbenes

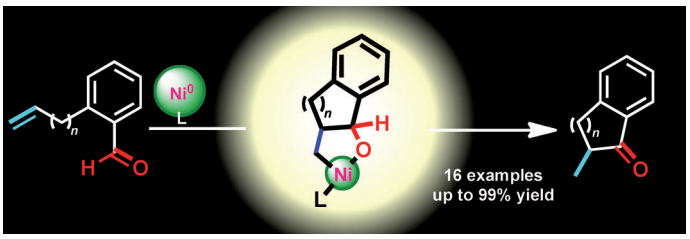

Getting some closure: Mechanistic studies supported the participation of an oxanickelacycle complex in the hydroacylation step of the title reaction, which proceeds without decarbonylation even in the absence of well-known chelation assistance by heteroatoms.

Heterocycles

I. Nakamura,* M. Okamoto, Y. Sato, M. Terada — 10816 – 10819

Synthesis of Azepine Derivatives by Rhodium-Catalyzed Tandem 2,3-Rearrangement/Heterocyclization

Front Cover

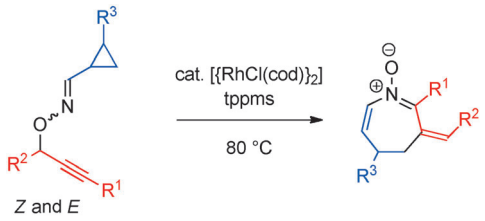

Easy to N-cycle: The efficient synthesis of azepine derivatives was achieved by Rh-catalyzed tandem 2,3-rearrangement involving the heterocyclization of *N*-allenylnitrone intermediates (see scheme; cod = 1,5-cyclooctadiene, tppms = sodium diphenylphosphinobenzene-3-sulfonate).

Natural Products

J. Wu, S. Tokuyama, K. Nagai, N. Yasuda, K. Noguchi, T. Matsumoto, H. Hirai, H. Kawagishi* — 10820 – 10822

Strophasterols A to D with an Unprecedented Steroid Skeleton: From the Mushroom *Stropharia rugosoannulata*

Skeletons in the closet: Four new compounds have been isolated from the title mushroom. The compounds display a new steroid skeleton (e.g., **1**) not previously reported for steroids. Preliminary bioactivity tests show that compound **1** can protect neuronal cells by attenuating the endoplasmic reticulum stress, and has weak anti-methicillin-resistant *Staphylococcus aureus* activity.

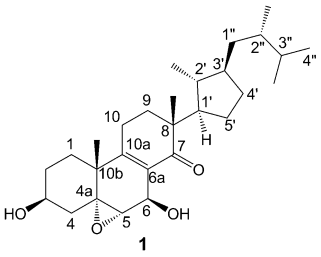

1

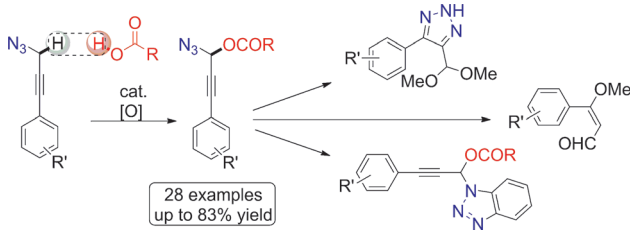

Hot couple: Propargyl azides were coupled with carboxylic acids by an iron-catalyzed dehydrogenative C–O bond formation (see scheme). This method enables propargylic C_{sp^3}–H functionalization under mild reaction conditions and also may involve the application of the azido moiety as an assisting group in C–H activation.

Dehydrogenative Coupling

T. Wang, W. Zhou, H. Yin, J.-A. Ma, N. Jiao* ——— **10823 – 10826**

Iron-Facilitated Oxidative Dehydrogenative C–O Bond Formation by Propargylic C_{sp^3}–H Functionalization

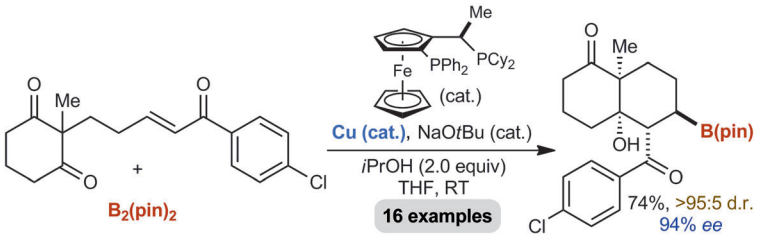

Piña colato? In the presence of a chiral Cu^{I}/bisphosphine complex and $B_2(pin)_2$, enone diones undergo diastereo- and enantioselective desymmetrization to deliver highly functionalized bicyclic products. The products can be used as substrates in additional transformations. pin = pinacolato, Cy = cyclohexyl.

Domino Reactions

A. R. Burns, J. Solana González, H. W. Lam* ——— **10827 – 10831**

Enantioselective Copper(I)-Catalyzed Borylative Aldol Cyclizations of Enone Diones

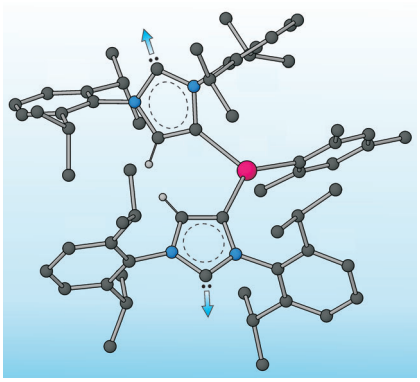

A tale of two carbenes: Reaction of :C[N(2,6-*i*Pr$_2$C$_6$H$_3$)CH]$_2$ (IPr) with Mn$_3$(mes)$_6$ (mes = 2,4,6-trimethylphenyl) yielded the trigonal planar complex [Mn(IPr)(mes)$_2$]. Reduction of this species with potassium/graphite in THF afforded the polymeric dicarbene-bridged species K[{:C[N(2,6-*i*Pr$_2$C$_6$H$_3$)]$_2$(CH)C}$_2$-Mn(mes)(thf)]·THF (see picture). The anionic moiety in this complex is the first reported example of a transition metal complex containing an N-heterocyclic dicarbene ligand. Gray C, blue N, red Mn.

NHC Complexes

R. A. Musgrave, R. S. P. Turbervill, M. Irwin, J. M. Goicoechea* ——— **10832 – 10835**

Transition Metal Complexes of Anionic N-Heterocyclic Dicarbene Ligands

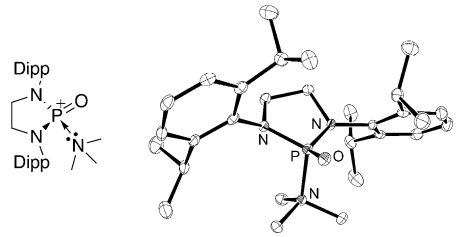

Totally OXOme! Monomeric oxophosphonium ions have been prepared from N-heterocyclic phosphenium ions and triethylamine or pyridine *N*-oxides (see picture; Dipp = 2,6-diisopropylphenyl). Their structures were confirmed by single-crystal X-ray crystallography.

Phosphorus Cations

A. D. Hendsbee, N. A. Giffin, Y. Zhang, C. C. Pye, J. D. Masuda* ——— **10836 – 10840**

Lewis Base Stabilized Oxophosphonium Ions

Structure Elucidation

C. Segarra, E. Mas-Marzá, M. Benítez, J. A. Mata, E. Peris* ____ 10841 – 10845

Unconventional Reactivity of Imidazolylidene Pyridylidene Ligands in Iridium(III) and Rhodium(III) Complexes

Expect the unexpected: The reactions of a series of imidazolium pyridinium salts with $[\{IrCp^*Cl_2\}_2]$ and $[\{RhCp^*Cl_2\}_2]$ afford a series of complexes. Together with the expected bis(NHC) complexes, some species resulting from C–C coupling between the pyridylidene and Cp* ligands were observed (see figure; Cp* = pentamethylcyclopentadienyl).

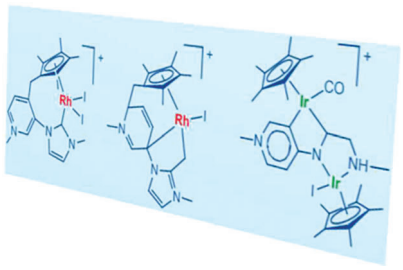

Natural Products

F.-M. Zhang, L. Peng, H. Li, A.-J. Ma, J.-B. Peng, J.-J. Guo, D. Yang, S.-H. Hou, Y.-Q. Tu,* W. Kitching ____ 10846 – 10850

Total Synthesis of the Nominal Didemnaketal A

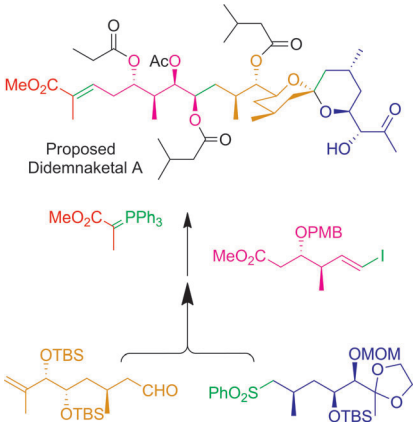

False identity: The synthesis of a natural product described by Faulkner and coworkers two decades ago has revealed the need for the revision of some stereochemical assignments. The key steps in this flexible route, which could provide access to stereodefined analogues for biological evaluation, included a Julia coupling, a Suzuki–Miyaura reaction, and Wittig olefination (see scheme; MOM, PMB, and TBS are protecting groups).

Synthetic Methodology

J. H. Lee, S. Gupta, W. Jeong, Y. H. Rhee,* J. Park* ____ 10851 – 10855

Characterization and Utility of N-Unsubstituted Imines Synthesized from Alkyl Azides by Ruthenium Catalysis

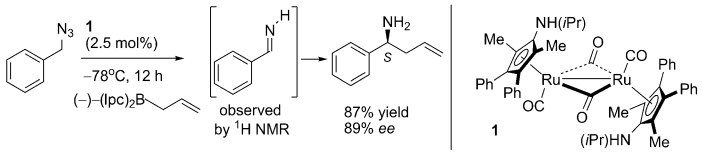

Shine a light: A fluorescent light-induced synthetic method for the title compounds has been developed and the chemoselective nature of the reaction is highlighted by the observation of the *cis*/*trans* isomers of various N-unsubstituted imines. The synthetic utility of this method is demonstrated by the one-pot imine formation/asymmetric allylation sequence of benzyl azide catalyzed by **1**. (Ipc = isopinocampheyl).

Asymmetric Synthesis

I. Cano, E. Gómez-Bengoa, A. Landa, M. Maestro, A. Mielgo, I. Olaizola, M. Oiarbide, C. Palomo* ____ 10856 – 10860

N-(Diazoacetyl)oxazolidin-2-thiones as Sulfur-Donor Reagents: Asymmetric Synthesis of Thiiranes from Aldehydes

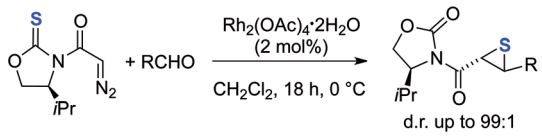

Sulfur tyranny: Thiiranes, instead of oxiranes, can be obtained in a highly stereoselective manner through the cycloaddition reaction of *N*-acyl oxazolidine tethered diazo thione compounds with aldehydes catalyzed by Rh^{II}. Thus, this reaction provides versatile adducts S functionalized at both the α and β position, with concomitant generation of two contiguous stereocenters.

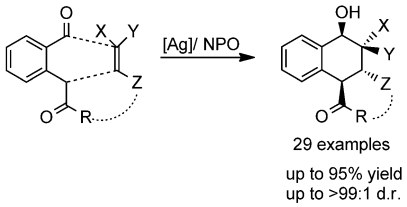

Silver bullet: A methodology for stereoselective synthesis of polysubstituted tetrahydronaphthols catalyzed by [Ag$^+$]/NPO has been developed. The reactions proceeded through an unprecedented [4+2] cyclization of 2-(2-formylphenyl)ethanone and an alkene, in both inter- and intramolecular fashion. NPO = pyridine *N*-oxide.

Synthetic Methods

S. F. Zhu,* R. X. Liang, H. F. Jiang, W. Q. Wu _____ **10861 – 10865**

An Efficient Route to Polysubstituted Tetrahydronaphthols: Silver-Catalyzed [4+2] Cyclization of 2-Alkylbenzaldehydes and Alkenes

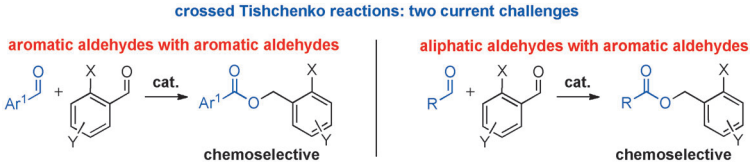

Crossed products: *Ortho*-substituted benzaldehydes react with other aromatic aldehydes in a highly selective, atom-economical Tishchenko disproportionation (see scheme) in the presence of a readily prepared, inexpensive thiolate-based catalyst. The methodology is of exceptionally wide scope and exhibits a high functional-group tolerance.

Homogeneous Catalysis

S. P. Curran, S. J. Connon* _____ **10866 – 10870**

The Thiolate-Catalyzed Intermolecular Crossed Tishchenko Reaction: Highly Chemoselective Coupling of Two Different Aromatic Aldehydes

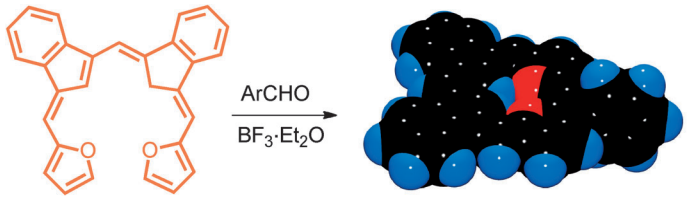

Porphyrin without N: Bilin analogues and related aromatic dicarbaporphyrinoids have been prepared from bis(3-indenyl)methane. Even though all four pyrrole rings from the porphyrin macrocycle have been replaced by two furan and two indene subunits, the system retains porphyrin-like UV/Vis spectra and highly diatropic characteristics.

Dicarbaporphyrinoids

T. D. Lash,* A. D. Lammer, G. M. Ferrence _____ **10871 – 10875**

Two-Step Synthesis of Stable Dioxadicarbaporphyrins from Bis(3-indenyl)methane

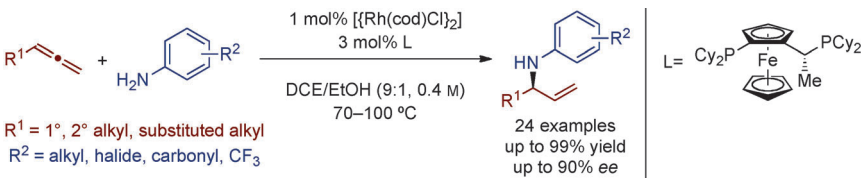

Branching out: The rhodium-catalyzed enantioselective hydroamination of monosubstituted allenes with anilines permits the atom-economic synthesis of valuable branched allylic amines. In contrast to previous linear selective allene hydroaminations, a Rh^I/Josiphos catalyst system (see scheme; cod = 1,5-cyclooctadiene, DCE = 1,2-dichloroethane) allows branched allylic amines to be obtained with perfect regioselectivity, high yield, and good enantioselectivity.

Asymmetric Catalysis

M. L. Cooke, K. Xu, B. Breit* _____ **10876 – 10879**

Enantioselective Rhodium-Catalyzed Synthesis of Branched Allylic Amines by Intermolecular Hydroamination of Terminal Allenes

B,N Heterocycles

S. A. Brough, A. N. Lamm, S.-Y. Liu, H. F. Bettinger* ——— 10880 – 10883

Photoisomerization of 1,2-Dihydro-1,2-Azaborine: A Matrix Isolation Study

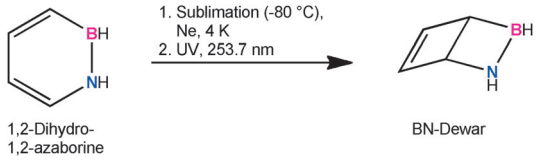

Closing the loop: Photoisomerization of 1,2-dihydro-1,2-azaborine in neon, argon, or xenon at 4 K with UV light (253.7 nm) as part of a matrix isolation study led to the Dewar form as the only photoproduct, in agreement with the vibrational spectra computed for possible isomers of 1,2-dihydro-1,2-azaborine.

Actinide Complexes

P. Hrobárik,* V. Hrobáriková, A. H. Greif, M. Kaupp* ——— 10884 – 10888

Giant Spin-Orbit Effects on NMR Shifts in Diamagnetic Actinide Complexes: Guiding the Search of Uranium(VI) Hydride Complexes in the Correct Spectral Range

Inside Cover

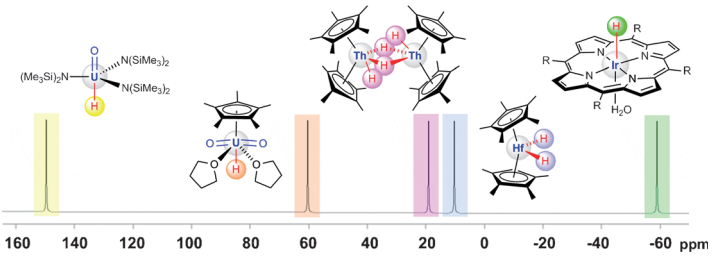

Looking in the right (NMR) ballpark: The ^{13}C shifts of carbon atoms σ-bonded to uranium(VI) centers, and in particular the ^{1}H shifts of U^{VI} bound hydride ligands, are predicted to be at unprecedentedly high frequencies (see picture), as a result of unexpectedly large spin-orbit effects. Based on relativistic quantum-chemical calculations, the right spectral ranges are suggested, which may allow identification of such compounds.

Natural Product Synthesis

K. Simon, J. Wefer, E. Schöttner, T. Lindel* ——— 10889 – 10892

Enantioselective Total Synthesis of the Diterpene (+)-Cubitene

From termite soldier's secretions: The enantioselective total synthesis of the diterpene (+)-cubitene is described. The route is characterized by the cyclization of a carvone-derived C_{20} allylphosphate with SmI_2, followed by fragmentation to the twelve-membered ring. As a result, perfect stereocontrol of the isopropenyl-substituted positions is achieved.

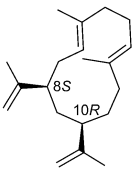

(+)-cubitene

Methanetrisamidines

B. Gutschank, S. Schulz,* M. Marcinkowski, G. Jansen, H. Bandmann, D. Bläser, C. Wölper ——— 10893 – 10897

Synthesis, Structure, Tautomerism, and Reactivity of Methanetrisamidines

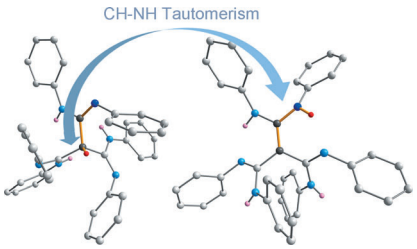

Tout au contraire: Both tautomeric forms of a methanetrisamidine were structurally characterized for the first time by X-ray diffraction and by ab initio calculations (see structures; gray C, red H, blue N). Their reactivity as proton acceptors and multianionic ligands was demonstrated.

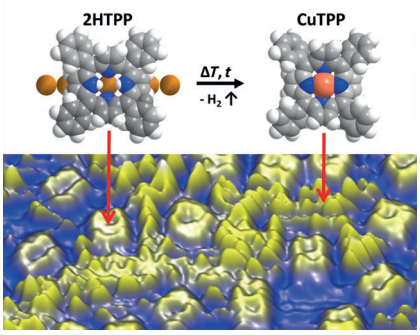

By simply counting individual molecules in STM images after defined heating steps, the kinetic parameters and the activation energy of a complex surface reaction can be determined quantitatively. This procedure was demonstrated for the metalation of 2H-tetraphenylporphyrin (2HTPP) with substrate atoms on a Cu-(111) surface.

Porphyrin Metalation

S. Ditze, M. Stark, M. Drost, F. Buchner, H.-P. Steinrück, H. Marbach* _____ **10898 – 10901**

Activation Energy for the Self-Metalation Reaction of 2H-Tetraphenylporphyrin on Cu(111)

Supporting information is available on www.angewandte.org (see article for access details).

A video clip is available as Supporting Information on www.angewandte.org (see article for access details).

This article is available online free of charge (Open Access).

This article is accompanied by a cover picture (front or back cover, and inside or outside).

Angewandte Corrigendum/Apology

The structure of compound **7** in Scheme 3 as well as in the graphical abstract of this Highlight is incorrect. The corrected structure is depicted here.

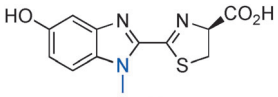

7

In order to be more accurate, the head of the right column in Table 1 has to be revised as follows (change in italics).

Table 1: Emission maxima for wild-type luciferase and Ultra-Glo with each luciferin substrate, as well as their applications in bioluminescence imaging.

Substrate	λ_{max} [nm]		Detection in vivo
	wild-type	Ultra-Glo	*or in cells*
...	...	...	...

Furthermore, in the published article some sentences were directly copied from the original articles. The authors sincerely apologize for this unprofessional behavior. Quotation marks around these sentences should be added in order to compensate for this mistake:

"Bioluminescence, the conversion of chemical energy into light ..." [16]

"... cells and tissues do not normally emit significant numbers ..." [7]

"noninvasive bioluminescence imaging of living subjects ..." [6]

"Despite its remarkable versatility, bioluminescence ..." [7]

[6] N. R. Conley, A. Dragulescu-Andrasi, J. Rao, W. E. Moerner, *Angew. Chem.* **2012**, *124*, 3406; *Angew. Chem. Int. Ed.* **2012**, *51*, 3350.

[7] D. C. McCutcheon, M. A. Paley, R. C. Steinhardt, J. A. Prescher, *J. Am. Chem. Soc.* **2012**, *134*, 7604.

[16] B. R. Branchini, M. H. Murtiashaw, R. A. Magyar, N. C. Portier, M. C. Ruggiero, J. G. Stroh, *J. Am. Chem. Soc.* **2002**, *124*, 2112.

D-Luciferin Analogues: a Multicolor Toolbox for Bioluminescence Imaging

Y.-Q. Sun, J. Liu, P. Wang, J. Zhang, W. Guo* _____ **8428–8430**

Angew. Chem. Int. Ed. **2012**, *51*

DOI: 10.1002/anie.201203565

Angewandte Addition

A Sinter-Resistant Catalytic System Based on Platinum Nanoparticles Supported on TiO_2 Nanofibers and Covered by Porous Silica

Y. Dai, B. Lim, Y. Yang, C. M. Cobley, W. Li, E. C. Cho, B. Grayson, P. T. Fanson, C. T. Campbell, Y. Sun, Y. Xia* ——— **8165–8168**

Angew. Chem. Int. Ed. **2010**, *49*

DOI: 10.1002/anie.201001839

The authors of this communication wish to add the following passage to their acknowledgement:
"A portion of the research was performed using EMSL, a national scientific user facility sponsored by the Department of Energy's Office of Biological and Environmental Research and located at Pacific Northwest National Laboratory."